

See discussions, stats, and author profiles for this publication at: <https://www.researchgate.net/publication/243374865>

# Temperature-Dependent Infrared Spectroscopy of Proton-Conducting Hydrated Perovskite $\text{BaIn}_x\text{Zr}_{1-x}\text{O}_{3-x/2}$ ( $x = 0.10-0.75$ )

ARTICLE in THE JOURNAL OF PHYSICAL CHEMISTRY C · APRIL 2010

Impact Factor: 4.77 · DOI: 10.1021/jp910307u

---

CITATIONS

3

---

READS

14

## 4 AUTHORS, INCLUDING:



**Maths Karlsson**

Chalmers University of Technology

38 PUBLICATIONS 344 CITATIONS

SEE PROFILE



**Aleksandar Matic**

Chalmers University of Technology

109 PUBLICATIONS 1,606 CITATIONS

SEE PROFILE



**Istaq Ahmed**

Chalmers University of Technology

23 PUBLICATIONS 365 CITATIONS

SEE PROFILE

# Temperature-Dependent Infrared Spectroscopy of Proton-Conducting Hydrated Perovskite $\text{BaIn}_x\text{Zr}_{1-x}\text{O}_{3-x/2}$ ( $x = 0.10\text{--}0.75$ )

Maths Karlsson,<sup>\*,†</sup> Aleksandar Matic,<sup>‡</sup> Ezio Zanghellini,<sup>‡</sup> and Istaq Ahmed<sup>§</sup>

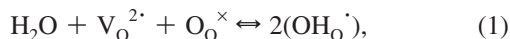
European Spallation Source Scandinavia, Lund University, SE-221 00 Lund, Sweden, Department of Applied Physics, and Department of Chemical and Biological Engineering, Chalmers University of Technology, SE-412 96 Göteborg, Sweden

Received: October 28, 2009; Revised Manuscript Received: February 5, 2010

We investigate the temperature dependence of the O–H stretch band in the infrared absorbance spectra of the proton-conducting hydrated perovskites  $\text{BaIn}_x\text{Zr}_{1-x}\text{O}_{3-x/2}$  ( $x = 0.10\text{--}0.75$ ) over the temperature range  $-160$  to  $350$  °C. Upon increasing temperature from  $-160$  to  $30$  °C, we show that there is a redistribution of protons from nonsymmetrical structural configurations, such as Zr–OH–In and Zr–OH–Zr–vacancy, where the degree of hydrogen bonding between the protons and neighboring oxygens is strong, to symmetrical configurations, such as Zr–OH–Zr and In–OH–In, where hydrogen bonding is weaker. Spectra measured at elevated temperatures,  $30\text{--}350$  °C, indicate preferential desorption of protons in sites where the degree of hydrogen bonding is strong, and show that the materials gradually dehydrate with increasing temperature. The dehydration rate is found to be highest in the temperature range  $275\text{--}325$  °C. Furthermore, the spectroscopic results indicate that strong hydrogen bonding, caused by dopant-induced short-range structural distortions, is favorable for high proton mobility and that the rate-limiting step in the conduction mechanism is the proton transfer between neighboring oxygens.

## 1. Introduction

Hydrated acceptor-doped perovskite-type oxides, of the form  $\text{ABO}_3$ , have been widely studied in recent years due to their high proton conductivities ( $\sim 10^{-3}\text{--}10^{-2}$  S  $\text{cm}^{-1}$ ) at intermediate temperatures ( $200\text{--}500$  °C) and concomitant promise for use as electrolytic membranes in fuel cells.<sup>1</sup> The acceptor-doping, such as In substituted for Zr in  $\text{BaZrO}_3$ , creates an oxygen-deficient structure. Protons can be introduced into this structure by exposure to humid conditions at elevated temperatures at which water molecules dissociate into hydroxide ions, which fill the oxygen vacancies, and protons, which bond to lattice oxygens, according to eq 1,



and shown schematically in Figure 1a. The protons are not stuck to any particular oxygens but are rather free to move from one oxygen to another, which results in the high proton conductivities observed in these materials.<sup>1</sup> However, the energy landscape for the protons is usually quite complex with several different sites in the structure with different potential energies and thus different local mobilities.

The proton conduction mechanism is generally believed to be divided into two elementary processes: (i) proton transfer between neighboring oxygens via hydrogen bonds and (ii) rotational motion of the hydroxyl group in between such transfers, see Figure 1b.<sup>1,2</sup> The rates of these processes are mutually coupled and sensitive to the local environment around

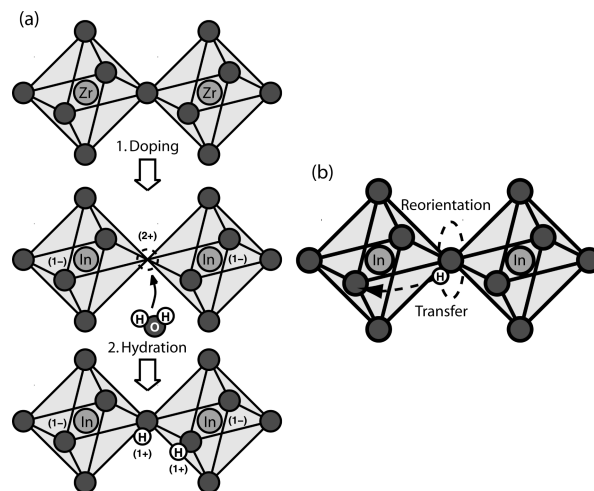


**Figure 1.** (a) Schematic picture of doping with  $\text{In}^{3+}$  to the  $\text{Zr}^{4+}$  site in cubic  $\text{BaZrO}_3$ , followed by the incorporation of protons through hydration in a humid atmosphere. (b) Illustration of the local dynamical steps in the proton conduction mechanism.

the proton, in particular to the degree of hydrogen bonding to a neighboring oxygen.<sup>1,3</sup> Strong hydrogen bonding increases the rate of proton transfer but suppresses the reorientational rate since this step requires breaking of such bonds. A thorough knowledge about the hydrogen bond interactions in this class of material is thus important for understanding the details of the proton transport.

Information about the hydrogen bonding in hydrated perovskites can be obtained from the O–H stretch vibrations, which are manifested as a strong and broad band in the infrared (IR) absorbance spectrum, usually between  $2800$  and  $3700$   $\text{cm}^{-1}$ ,<sup>3,4</sup> although it should be noted that bands with frequencies lower than  $2000$   $\text{cm}^{-1}$  have also been assigned to fundamental O–H

\* To whom correspondence should be addressed. E-mail: maths.karlsson@esss.se.

<sup>†</sup> Lund University.

<sup>‡</sup> Department of Applied Physics, Chalmers University of Technology.

<sup>§</sup> Department of Chemical and Biological Engineering, Chalmers University of Technology.

stretch modes.<sup>5</sup> This may be compared to the pure O–H stretch frequency for the non-hydrogen-bonded water molecule, which is found as a narrow band at  $3657\text{ cm}^{-1}$ .<sup>6</sup> The down-shift of the O–H stretch band in the spectra of hydrated perovskites is a consequence of hydrogen bond interactions between the protons and neighboring oxygens, which result in an increase of the O–H bond length and hence lowers the vibrational frequency. The broad nature of the O–H stretch band is due to a wide distribution of degrees of hydrogen bonding (hydrogen bond strengths) in the material.

In a combined experimental and theoretical study of In-doped BaZrO<sub>3</sub> we have previously shown that the different parts of the O–H stretch region can be related to certain configurations of the protons in the structure.<sup>3</sup> The high-frequency part can be associated to protons in relatively symmetrical environments, such as In–OH–In and Zr–OH–Zr, where the degree of hydrogen bonding is weak and the O–H stretch vibrational frequency high. In contrast, the low-frequency part of the O–H stretch region is related to protons located in relatively nonsymmetrical configurations, such as In–OH–Zr or Zr–OH–Zr–vacancy, with an enhanced tendency for strong hydrogen-bond formation.<sup>3</sup> In particular, very low-frequency bands,  $< 2500\text{ cm}^{-1}$ , have been suggested to originate from protons in structurally distorted local environments induced by dopant atoms and/or oxygen vacancies.<sup>3</sup> The presence of dopant-induced local structural distortions in the same materials was recently revealed by vibrational spectroscopy.<sup>7</sup> In that work, it was also found that the structural distortions become more pronounced with increasing dopant level.<sup>7</sup>

In this paper we investigate the temperature dependence of the O–H stretch band for the proton-conducting hydrated perovskites BaIn<sub>x</sub>Zr<sub>1–x</sub>O<sub>3–x/2</sub> ( $x = 0.10, 0.25, 0.50$ , and  $0.75$ ). The temperature dependence of the O–H stretch band gives information not only about the hydration/dehydration behavior of the material but also about the protons' potential energy landscape in the structure. Nevertheless, there is, to the best of our knowledge, apart from one study that focuses on the IR spectra of hydrated Y-doped BaCeO<sub>3</sub> at  $-269$  and  $30\text{ °C}$  and that reveals a sharpening of the O–H stretch band at the lower temperature,<sup>8</sup> no other reported work on this topic in the literature.

The BaIn<sub>x</sub>Zr<sub>1–x</sub>O<sub>3–x/2</sub> system has been widely studied by us by means of vibrational spectroscopy,<sup>3,7,9</sup> X-ray and neutron diffraction, and impedance spectroscopy.<sup>10–12</sup> It has an average cubic structure (space group  $Pm\bar{3}m$ ) for the chosen dopant concentrations.<sup>10,11,13–15</sup> Thus, the choice of system enables a systematic investigation of the temperature dependence of the hydrogen bond characteristics as a function of temperature and dopant concentration with the overall cubic structure preserved.

## 2. Experimental Methods

**A. Sample Preparation.** Samples of BaIn<sub>x</sub>Zr<sub>1–x</sub>O<sub>3–x/2</sub> ( $x = 0.10, 0.25, 0.50$ , and  $0.75$ ) were prepared through traditional solid state sintering.<sup>10,11</sup> The oxygen-deficient perovskite powders were hydrated at  $250\text{--}300\text{ °C}$  in a flow of N<sub>2</sub> saturated at  $76.2\text{ °C}$  with water vapor for a period over a week. Thermal gravimetric analyses (TGA) on In-doped BaZrO<sub>3</sub> show hydration levels in the range  $\sim 60\text{--}90\%$ ,<sup>10,15</sup> and data from inelastic neutron scattering suggests that the degree of hydration is largely independent of the In concentration.<sup>9</sup>

**B. Infrared Spectroscopy.** Infrared spectra were measured over the region  $1700\text{--}4500\text{ cm}^{-1}$  with a Bruker IFS 66v/s FT-IR spectrometer equipped with a MCT (Mercury Cadmium Telluride) detector and a KBr beam splitter. Temperature-

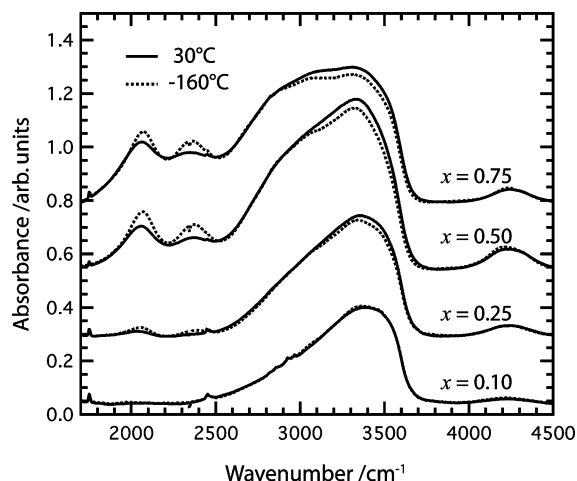


**Figure 2.** Infrared spectra of hydrated BaIn<sub>x</sub>Zr<sub>1–x</sub>O<sub>3–x/2</sub> ( $x = 0.10\text{--}0.75$ ) at  $30$  and  $-160\text{ °C}$ .

dependent measurements were performed in diffuse reflectance mode, using the diffuse reflectance device Praying Mantis and the low-temperature reaction chamber CHC–CHA from Harrick<sup>16</sup> cooled with liquid nitrogen. The sample chamber of the spectrometer was reconstructed to have the Praying Mantis device under vacuum during the measurements, in which water absorption from air on the sample was avoided and the signal-to-noise ratio was improved. The vacuum was found to have no effect on the spectra, thus neither on the proton concentration in the sample. For all materials, spectra were measured at  $30$  and  $-160\text{ °C}$ , while for the  $x = 0.50$  and  $0.75$  compositions spectra were also measured at  $100, 150, 200, 225, 250, 275, 300, 325$ , and  $350\text{ °C}$ . The measured spectra are averaged over 500 scans with a resolution of  $2\text{ cm}^{-1}$ .

Consecutive measurements were performed at each temperature to make sure that the spectra, which are presented in this paper, were recorded under equilibrium conditions. Spectra of a wrinkled Al-foil, recorded at each temperature, were used as reference spectra. Absorbance-like spectra of the samples were derived by taking the logarithm of the ratio between the reference spectra and the corresponding sample spectra.

## 3. Results and Discussion

**A. Spectra at  $30$  and  $-160\text{ °C}$ .** Figure 2 shows the IR spectra for the hydrated cubic-structured perovskites BaIn<sub>x</sub>Zr<sub>1–x</sub>O<sub>3–x/2</sub> ( $x = 0.10, 0.25, 0.50$ , and  $0.75$ ) measured at  $30$  and  $-160\text{ °C}$ . The spectra for all compositions display a broad O–H stretch band between  $2500$  and  $3700\text{ cm}^{-1}$ ,<sup>3</sup> and a less intense band at around  $4250\text{ cm}^{-1}$ , which most likely is related to a combination of a O–H stretch and a O–H wag mode.<sup>9</sup> In addition, we observe two bands at  $2050$  and  $2350\text{ cm}^{-1}$  for  $x \geq 0.25$ . These bands have been proposed to be related to O–H stretch vibrations with the protons located in environments which locally deviate significantly from the average cubic symmetry of the perovskite lattice.<sup>3</sup> The structural distortions are introduced by the In-doping and create proton sites with an enhanced degree of hydrogen bonding, thus lowering the O–H stretch frequency.<sup>3,7</sup> The fact that the  $2050$  and  $2350\text{ cm}^{-1}$  bands cannot be discerned for  $x = 0.10$ , and are very weak for  $x = 0.25$ , is a consequence of the distortions being weak and the number of nonsymmetrical sites being quite limited at this relatively low dopant level.

In a transient inspection of Figure 2 one observes that the spectra measured at the two different temperatures are overall similar to each other, regardless of the In concentration. In

particular, the spectra of the  $x = 0.10$  material are more or less identical. However, for  $x \geq 0.25$ , we observe that the low-temperature spectra clearly show a higher intensity for the two low-frequency bands at 2050 and 2350  $\text{cm}^{-1}$ , and a lower intensity of the high-frequency part, 3000–3500  $\text{cm}^{-1}$ . This intensity redistribution observed for  $x \geq 0.25$  reflects a redistribution of the average population of protons between different structural configurations. In particular, the spectra suggest a redistribution from symmetrical sites, such as In-OH-In and Zr-OH-Zr, to less symmetrical sites, such as In-OH-Zr and/or Zr-OH-Zr-vacancy, when the temperature is lowered from 30 to  $-160$   $^{\circ}\text{C}$ . Since the Boltzmann distribution favors low-energy sites with decreasing temperature, this suggests that nonsymmetrical structural configurations, i.e., proton sites in the vicinity of dopant atoms and/or oxygen vacancies, have a lower potential energy than symmetrical configurations. This confirms the picture proposed by several independent first-principles calculations, which show that the potential energy landscape for the proton is significantly lowered in the vicinity of a dopant atom.<sup>17–20</sup>

**B. Spectra at 30–350  $^{\circ}\text{C}$ .** Figure 3 shows the spectra measured at temperatures in the range 30–350  $^{\circ}\text{C}$  for the concentrations  $x = 0.50$  and 0.75. For both materials we observe a gradual decrease in intensity over the whole O–H stretch region (1700–4500  $\text{cm}^{-1}$ ) as the temperature is increased. To quantitatively assess these changes we performed a peak fit analysis of the spectra.

The full spectra (1700–4000  $\text{cm}^{-1}$ ) were reproduced by six Gaussian bands, of which two Gaussians represent the 2050 and 2350  $\text{cm}^{-1}$  bands (I and II), while the other four (III–VI) represent the broad band in between 2500 and 3700  $\text{cm}^{-1}$ , following the analysis in ref 3. As an example, the fit of the  $T = 30$   $^{\circ}\text{C}$  spectrum for  $x = 0.75$  is shown in Figure 3c. To obtain reasonable fits, consistent between the different temperatures, we fixed the positions and widths of bands I and II to the values obtained from the fit of the spectra at 30  $^{\circ}\text{C}$ . It was found that neither the positions nor the widths of bands III–VI exhibited any temperature dependence within error bars. The temperature dependence of the (i) integrated intensity of each Gaussian band relative to the total integrated intensity of the six Gaussian bands (the total intensity) and the (ii) total integrated intensity at each temperature normalized to the total integrated intensity at 30  $^{\circ}\text{C}$  are shown in Figure 4 for the two materials.

From Figure 4 it is clear that the total intensity of the O–H stretch region decreases gradually with increasing temperature for both materials, and that the decrease is more continuous for the  $x = 0.50$  material compared to  $x = 0.75$ . As the intensity of the O–H stretch band is related to the concentration of protons in the structure, these results imply that the concentration of protons becomes successively lower with increasing temperature, i.e., the materials gradually dehydrate. The dehydration rate is highest in the temperature range 275–325  $^{\circ}\text{C}$ , which is in good agreement with TGA data as reported for  $x = 0.50$ .<sup>21</sup>

Furthermore, Figure 4 reveals a change in the shape of the spectrum as the temperature is increased. Most important, we can see a clear diminishing of the relative intensity of the low-frequency part of the O–H stretch band (bands I and II) and an increase of the relative intensity of the corresponding high-frequency part (bands IV and V), while the relative intensity of the middle band (III) only slightly decreases with temperature and the highest frequency band (VI) is basically unchanged. At high temperature (275  $^{\circ}\text{C}$  for  $x = 0.50$  and 325  $^{\circ}\text{C}$  for  $x = 0.75$ ), the two low-frequency bands (I and II) can no longer be

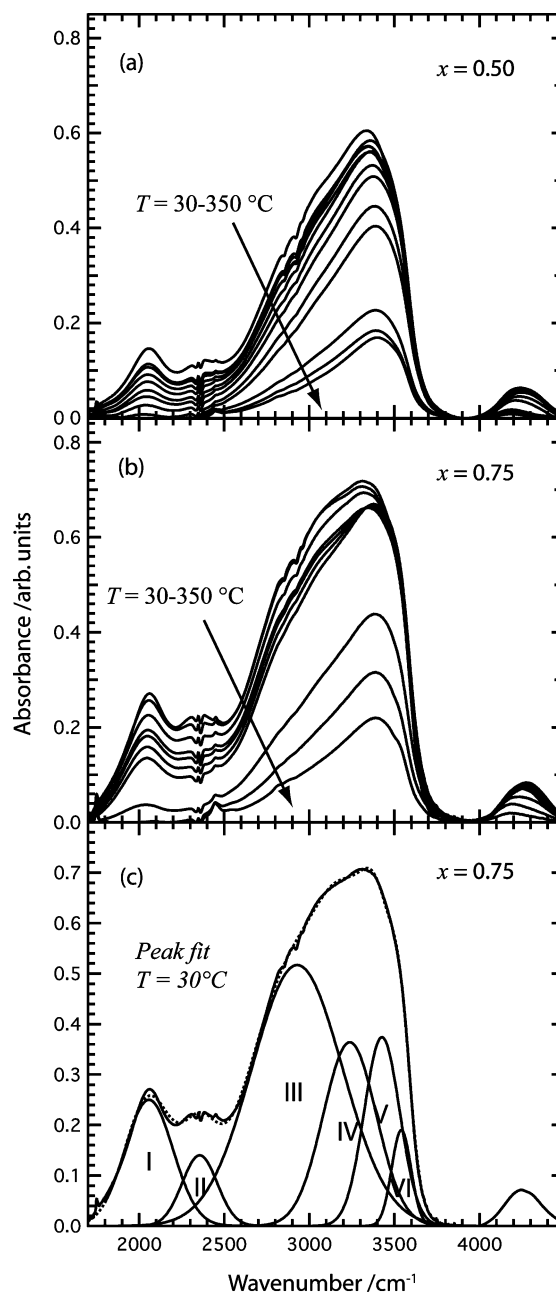


**Figure 3.** (a, b) Infrared spectra of hydrated  $\text{BaIn}_x\text{Zr}_{1-x}\text{O}_{3-x/2}$  ( $x = 0.50$  and 0.75) for the temperatures 30, 100, 150, 200, 225, 250, 275, 300, 325, and 350  $^{\circ}\text{C}$ . (c) Peak fit for the 30  $^{\circ}\text{C}$  spectrum of  $x = 0.75$  with six Gaussian bands.

resolved, and all remaining intensity is now in the broad main band between 2500 and 3700  $\text{cm}^{-1}$ .

The redistribution of relative intensity from bands I and II to bands IV and V upon increasing temperature is in agreement with the spectra at  $-160$  and 30  $^{\circ}\text{C}$  (cf. Figure 2). However, this may not necessarily be related to a redistribution of protons from strongly hydrogen bonding sites to less hydrogen bonding sites since the materials are successively dehydrated. It may instead be related to preferential desorption of protons in those sites where the degree of hydrogen bonding is high. In turn, this result suggests that the most strongly hydrogen-bonded protons are also the most mobile protons in the structure. Thus, it appears that nonsymmetrical configurations of the protons, created by dopant-induced short-range structural distortions, are, in contrast to what often has been suggested, not detrimental but rather favorable for high proton mobility in hydrated



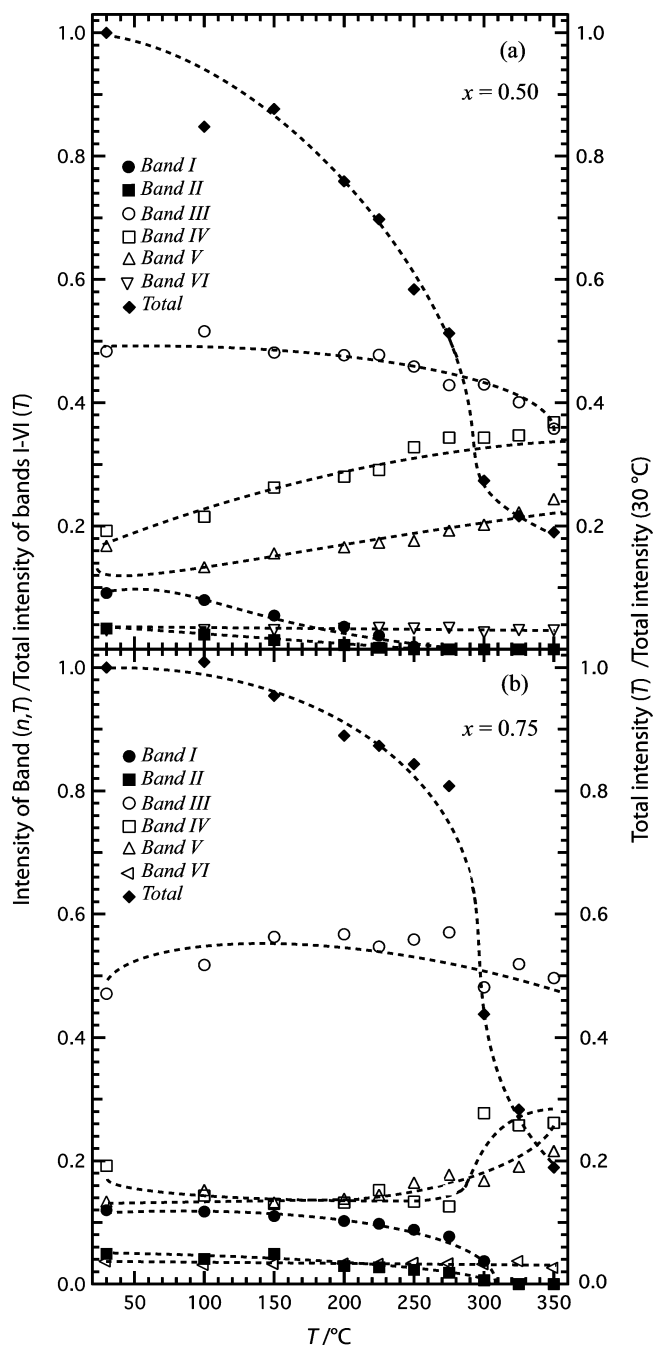


**Figure 4.** Left axis: Integrated intensities of the Gaussian bands (marked I–VI) relative to the total integrated intensity of the O–H stretch region ( $1700\text{--}4000\text{ cm}^{-1}$ ). Right axis: Total integrated intensity of the O–H stretch region normalized to the total integrated intensity at  $30\text{ }^{\circ}\text{C}$ . The dashed lines serve as guides to the eye.

perovskites. In this scenario the proton transfer between neighboring oxygens is then the rate-limiting step in the conduction process since it is favored by strong hydrogen bonding while the rotational motion of the  $\text{—OH}$  group is hindered as it requires the breaking of such bonds. We note that, at temperatures above  $\sim 300\text{ }^{\circ}\text{C}$ , where bands I and II are gone, the most mobile protons left in the structure are hence likely those related to band III, i.e., those which experience an “intermediate” degree of hydrogen bonding.

The fact that strong hydrogen bonding is favorable for fast proton mobility is consistent with the virtually temperature-independence of the relative intensity of band VI, which is related to the most weakly hydrogen bonded, thus least mobile,

protons in the structure. Here one should note that at this high doping level (50–75%) the average cubic structure possesses pronounced short-range structural distortions which are distributed throughout the entire perovskite lattice,<sup>7</sup> implying that the number of weakly hydrogen bonding sites is quite limited. A plausible explanation for the non-negligible intensity of band VI may thus be that it is related to protons located in the grain boundaries. Since the concentration of grain boundaries can be expected to be similar in the two samples, this suggestion is supported by the fact that the relative intensity of band VI seems concentration independent, see Figure 4.

#### 4. Conclusions

We have investigated the temperature dependence of the O–H stretch band in the infrared absorbance spectra of the cubic-structured hydrated perovskites  $\text{BaIn}_x\text{Zr}_{1-x}\text{O}_{3-x/2}$  ( $x = 0.10\text{--}0.75$ ), over the temperature range  $-160$  to  $350\text{ }^{\circ}\text{C}$ . We find that upon increasing temperature, from  $-160$  to  $30\text{ }^{\circ}\text{C}$ , there is a redistribution of protons from nonsymmetrical structural configurations, where the degree of hydrogen bonding is strong, to more symmetrical configurations, where the hydrogen bonding is weaker. Spectra measured at elevated temperatures,  $30\text{--}350\text{ }^{\circ}\text{C}$ , show a change in relative intensity of the different parts of the O–H stretch band as the temperature is increased, which is attributed to preferential desorption of protons in strongly hydrogen bonding configurations, but also that the total intensity decreases gradually as a result of a dehydration of the material. The dehydration rate is highest in the temperature range  $275\text{--}325\text{ }^{\circ}\text{C}$ , and it is found that the intensity of the bands related to strongly hydrogen bonding configurations shows the fastest decrease with increasing temperature, suggesting that strong hydrogen bonding is favorable for high proton mobility. Since it can be expected that strong hydrogen bonding is favorable for the proton transfer process but detrimental for the reorientational process in the proton conduction mechanism, our findings hence suggest that the proton transfer event is rate-limiting.

Finally, we conclude that infrared spectroscopy experiments over a wide temperature range, measurements that have been largely neglected for studies of hydrated perovskites before, not only can give accurate information about the dehydration process, but can also provide information about the protons’ potential energy landscape in the perovskite structure as well as the proton mobility. Such knowledge is important for further understanding of the proton transport in these materials, which is crucial for guidance of the preparation of new compounds with improved proton conductivities.

**Acknowledgment.** This work was supported by the Swedish Research Council (VR) and the Swedish National Graduate School in Materials Science (NFSM).

#### References and Notes

- (1) Kreuer, K. D. *Annu. Rev. Mater. Res.* **2003**, *33*.
- (2) Kreuer, K. D. *Chem. Mater.* **1996**, *8*, 610–641.
- (3) Karlsson, M.; Björketun, M. E.; Sundell, P. G.; Matic, A.; Wahnström, G.; Engberg, D.; Börjesson, L.; Ahmed, I.; Eriksson, S. G.; Berastegui, P. *Phys. Rev. B* **2005**, *72*, 094303.
- (4) Kreuer, K. D. *Solid State Ionics* **1997**, *97*, 1.
- (5) Omata, T.; Takagi, M.; Otsuka-Yao-Matsuo, S. *Solid State Ionics* **2004**, *168*, 99.
- (6) Lock, A. J.; Bakker, H. J. *J. Chem. Phys.* **2002**, *117*, 1708.
- (7) Karlsson, M.; Matic, A.; Knee, C. S.; Ahmed, I.; Börjesson, L.; Eriksson, S. G. *Chem. Mater.* **2008**, *20*, 3480.
- (8) Kreuer, K. D.; Münch, W.; Ise, M.; He, T.; Fuchs, A.; Traub, U.; Maier, J. *Ber. Bunsen-Ges.* **1997**, *101*, 1344.

- (9) Karlsson, M.; Matic, A.; Parker, S. F.; Ahmed, I.; Börjesson, L.; Eriksson, S. G. *Phys. Rev. B* **2008**, 77, 104302.
- (10) Ahmed, I.; Eriksson, S. G.; Ahlberg, E.; Knee, C. S.; Berastegui, P.; Johansson, L. G.; Rundlöf, H.; Karlsson, M.; Matic, A.; Börjesson, L.; Engberg, D. *Solid State Ionics* **2006**, 177, 1395.
- (11) Ahmed, I.; Eriksson, S. G.; Ahlberg, E.; Knee, C. S.; Karlsson, M.; Matic, A.; Engberg, D.; Börjesson, L. *Solid State Ionics* **2006**, 177, 2357.
- (12) Ahmed, I.; Knee, C. S.; Karlsson, M.; Eriksson, S. G.; Henry, P. F.; Matic, A.; Engberg, D.; Börjesson, L. *J. Alloys Compd.* **2008**, 450, 103.
- (13) Goodenough, J. B.; Ruiz-Diaz, J. E.; Zhen, Y. S. *Solid State Ionics* **1990**, 44, 21.
- (14) Manthiram, A.; Kuo, J. F.; Goodenough, J. B. *Solid State Ionics* **1990**, 62, 225.
- (15) Kreuer, K. D.; Adams, S.; Münch, W.; Fuchs, A.; Klock, U.; Maier, J. *Solid State Ionics* **2001**, 145, 295.
- (16) <http://www.harricksci.com> (accessed October 26, 2009).
- (17) Björketun, M. E.; Sundell, P. G.; Wahnström, G. *Phys. Rev. B* **2007**, 76, 054307.
- (18) Davies, R. A.; Islam, M. S.; Gale, J. D. *Solid State Ionics* **1999**, 126, 323.
- (19) Islam, M. S.; Davies, R. A.; Gale, J. D. *Chem. Mater.* **2001**, 13, 2049.
- (20) Islam, M. S.; Slater, P. R.; Tolchard, J. R.; Dinges, T. *Dalton Trans.* **2004**, 3061–3066.
- (21) Ahmed, I.; Eriksson, S. G.; Ahlberg, E.; Knee, C. S. *Solid State Ionics* **2008**, 179, 1155.

JP910307U